Synthesis, Spectral, Thermal and DPPH Scavenging Studies of the Hydrazone Derived Transition Metal Complexes

[1]Muhammad Ikram*, [1]Sadia Rehman**, [2]Muhammad Ayaz, [2]Syed Muhammad Salman, [1]Farzia, [2]Muhammad Imran, [3]Mutasem Omar Sinnokrot, [1]Farman Ullah, [4]Bushra Khan
[1]*Department of Chemistry, Abdul Wali Khan University Mardan, Pakistan.*
[2]*Department of Chemistry, Islamia College University Peshawar.*
[3]*Department of Chemistry, The Petroleum Institute, Khalifa University of Science and Technology, Abu Dhabi, 2533 United Arab Emirates.*
[4]*Department of Biochemistry, Abdul Wali Khan University Mardan, Pakistan.*
ikram@awkum.edu.pk*, sadia@awkum.edu.pk**

(Received on18th November 2019, accepted in revised form 11th August 2020)

Summary: Schiff base ligand 2,2-{benzene-1,4-diylbis[(E)methylylidene(1E,2E)hydrazine-2,1-diylidene(E)methylidene]}diphenol (H_2-BHMD) was synthesized by reacting together the ortho vaniline and 1,4-*bis*(hydrazonomethyl)benzene. It was characterized by analytical and spectroscopic techniques including ^{1}H-NMR, elemental analysis, FT-IR, and UV-Visible studies. Different transition metal ions like Co (II), Ni (II), Cu (II) and Zn (II) were reacted with well characterized ligand to obtain the metal derivatives. AAS, elemental analysis, FT-IR, molar conductance and UV-Visible methods were used to study the metal complexes. The analytical and spectroscopic technique suggested the formation of coordination polymers. The FT-IR results confirmed the bidentate binding of the ligand involving phenolic oxygen and azomethine nitrogen. The UV-visible studies suggested the formation of distorted square planar geometries for all the metal complexes. Hydrazone Schiff bases are known for their antioxidant activity, therefore the synthesized hydrazone and the corresponding metal complexes were also studied for their antioxidant capabilities utilizing DPPH free radicals. Among all complexes, the Co-BHMD demonstrated noteworthy percent hindrance to the free radicals, yet much lower than the standard medication utilized. The metal subsidiaries were likewise studied for their thermal degradation. The respective TG bands were utilized for dynamic and thermodynamic parameters estimation utilizing Horowitz-Metzger strategy.

Key words: Hydrazone Schiff base, metal complexes, spectroscopy, free radicals, kinetic and thermodynamic studies

Abbreviations: 2,2-{benzene-1,4-diylbis[(E)methylylidene(1E,2E)hydrazine-2,1-diylidene(E)methylidene]}diphenol (H_2-BHMD), Metal complexes of 2,2-{benzene-1,4-diylbis[(E)methylylidene(1E,2E)hydrazine-2,1-diylidene (E)methylidene]}diphenol (M-BHMD),

Introduction

Schiff bases are well known compounds because of their outstanding application in various fields like biological, medicinal, agriculture etc [1]. These outstanding compounds could be formed from reaction between primary amines and aldehydes/ketones (condensation reaction). Schiff bases are known for their complexation with various metal ions because of the -C=N- moiety (azomethine group) [2]. Chiral as well as achiral Schiff base ligands have been reported but chiral Schiff bases received considerable attention because it plays important role in the asymmetric epoxidation of unfunctionalized olefins [3].

The Schiff bases are also intermediates for the preparation of broad spectrum antibiotics like beta lactam [4, 5]. The metal complexes having Schiff base as a ligand attracted the attention of the chemists due to their wide biological role like antibacterial, antioxidant, and antitumor properties etc. It is well known that some Schiff bases show higher activities when administered as metal complexes [5-7].

Because of their importance, we synthesized a new Schiff base 2,2-{benzene-1,4-diylbis[(E)methylylidene(1E,2E)hydrazine-2,1-diylidene(E)methylidene]}diphenol ligand (H_2-BHMD) and its metal complexes (M-BHMD). Furthermore, the antioxidant properties, thermal degradation at different heating rates, ^{1}H-NMR, UV-Visible and atomic absorption spectroscopy (AAS) of the free ligand and complexes were studied. The obtained data from TG curve were treated mathematically for the determination of activation energies and activation enthalpies using the Horowitz-Metzger method [8].

*To whom all correspondence should be addressed.

Experimental

Instrumentation

Bruker 500 MHz spectrophotometer was used for recording ^{1}HNMR spectrum of H_2-BHMD ligand, with tetramethylsilane (TMS) as internal standard. PerkinElmer spectrum version 10.5.1 was used for recording FT-IR spectra of H_2-BHMD ligand and its metal complexes. Bibby scientific limited smp 10 instrument was used for recording the melting point of 1,4-*bis*(hydrazonomethyl)benzene, ligand H_2-BHMD and its metal complexes. The metal content of complexes (Co, Ni, Cu and Zn) were determined by using AAS PerkinElmer analyst 700. The UV-Vis spectra of the ligand H_2-BHMD and its metal complexes were recorded on BMS UV-1602. Fresh solution at room temperature has been used for all measurements. UV-Vis spectronic 2100 instrument was used for absorbance of complexes in antioxidant activity.

Chemical and reagent

Benzene-1,4-dicarbaldehyde, o-vaniline and hydrazine monohydrate were obtained from local suppliers of Sigma Aldrich and used as such without further purification. The metal acetate i.e. $M(CH_3COO)_2$. nH_2O (where M=Co, Ni, Cu and Zn), were obtained in hydrated form from Riedal-de-Haen. The metal acetate salts were dehydrated by keeping them in oven for 2-3 hours at 100 °C. Organic solvents methanol, dimethylsulfoxide (DMSO) and Tetrahydrofuran (THF) were obtained from local suppliers and standard procedures have been used for purification of these solvents.

Synthesis of 1,4-bis(hydrazonomethyl)benzene

1,4-*bis*(hydrazonomethyl)benzene is a building block molecule for preparation of Schiff base ligand. The 1,4-*bis*(hydrazonomethyl)benzene was synthesized by reacting together Benzene-1,4-dicarbaldehyde and hydrazine monohydrate in 2:1 molar ratio using methanol as a solvent. The resultant solution was stirred for 4-5 h at room temperature. The product was yellow solid which was obtained by concentrating the reaction mixture in rotary evaporator. The synthetic pathway is given in scheme 1.

Synthesis of 2,2-{benzene-1,4-diylbis[(E)methylylidene(1E,2E)hydrazine-2,1-diylidene-(E)-methylidene]}diphenol Schiff base ligand (H_2-BHMD)

Hydrated methanol was used for complete dissolution of 0.5g (0.00328 mol) 1,4-*bis*(hydrazonomethyl)benzene. Another fresh solution of 1g (0.0065 mol) o-vaniline was prepared by dissolving it in minimum quantity of methanol and acidified by the addition of 2mL acetic acid. The resulting solution was added dropwise on stirring to the solution of 1,4-*bis*(hydrazonomethyl)benzene and the reaction mixture was refluxed for 4-5 hours. Considerable amount of the product was isolated as yellow solid (Scheme 2).

Yield: 1g, 75 %. Elemental analysis; $C_{24}H_{22}O_4N_4$, Calc. C (66 %), N (13 %), O (14.86 %), H (5.15 %), Exp. C (66.89 %), N (13 %), O (14.86 %), H (5.14 %). IR: 3300 (vw), 2939.77 (w), 1699.04 (w), 1618 (s), 1460.70 (s), 1407.5 (m), 1319.89 (m), 1247.89 (s), 1078 (s), 955.59 (s), 833.14 (s), 779.58 (s), 733.57 (s), 534 (w), 520 (s) cm^{-1}. ^{1}HNMR (DMSO-d^6, 300 k, 500 MHz): 3.82 (s, -OCH_3), 6.91 (t, Aromatic CH, J = 8 Hz), 7.16 (d, Aromatic CH, J = 8 Hz), 7.29 (d, Aromatic CH, J = 8 Hz), 7.54 (s, Aromatic CH), 8.60 (s, -C=N), 13.04 (s, -OH). UV/ Vis: 220 nm, 230 nm, 340nm, 350nm, 370nm.

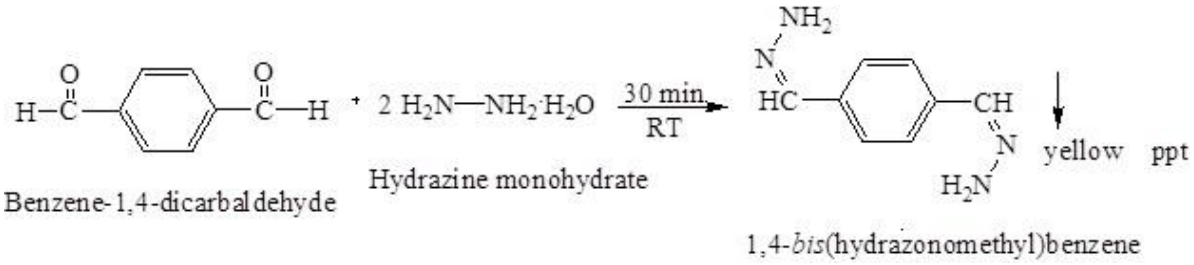

Scheme-1: Synthesis of 1,4-bis(hydrazonomethyl)benzene.

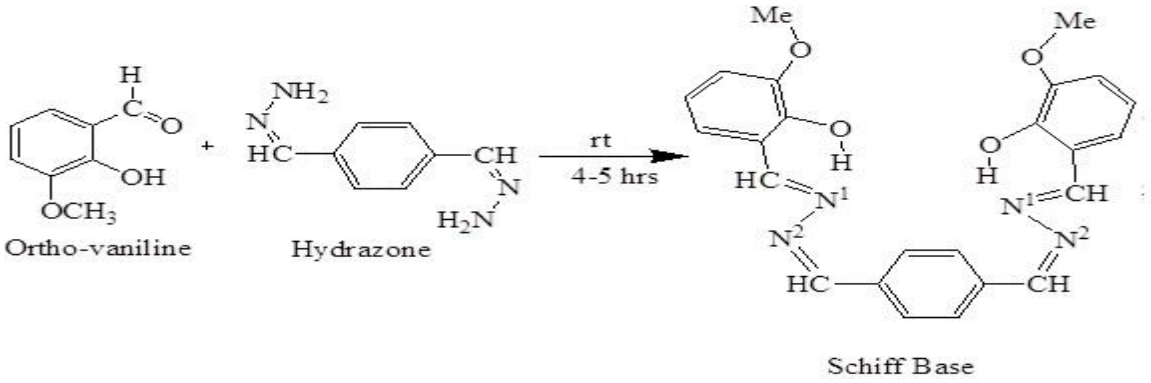

Scheme-2: Synthesis of H2-BHMD Schiff base ligand.

[1]HNMR spectroscopic confirmation

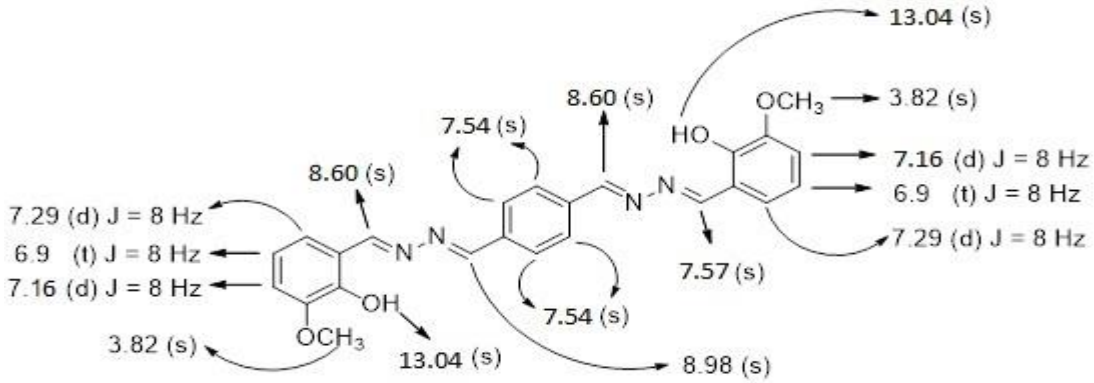

Fig. 1: [1]H-NMR assignment of H_2-BHMD Schiff base ligand.

Synthesis of metal complexes

The prepared Schiff base (H_2-BHMD) and hydrated metal acetate salt were taken in 2:1 molar ratio. 10cm^3 tetrahydrofuran solvent was used for the complete dissolution of 0.3gm Schiff base. The hydrated metal salt (0.07gm) $M(CH_3COO)_2$. nH_2O (where M^{2+} = Co, Zn, Ni and Cu) was dissolved in 10 cm^3 methanol. The two solutions were mixed together and stirred at 60-65 ˚C temperature for 4-5 h. The solution was left overnight then the product was collected after filtering the solution or obtained through rotary evaporator after concentrating the solution (Scheme 3).

Synthesis of Di[{2,2-{benzene-1,4-diylbis[(E)methylylidene(1E,2E)hydrazine-2,1-diylidene (E)methylidene]} diphenolatecobalt(II)] (Co-BHMD)

Yield: 73%. Elemental analysis; $C_{48}H_{42}CoN_8O_8$ (M.Wt: 917.266), Calc. C (62.79 %), N (12 %), O (13.95 %), H (4.1 %), Exp. C (62 %), N (12.50 %), O (13 %), H (4.5 %). FTIR: 3398.57 (b), 2954.95 (w), 1622.13 (w), 1602.85 (w), 1456 (w), 1435 (w), 1242 (s), 1213 (s),1166 (m), 1080 (w), 1014 (s), 952 (s), 738 (s), 520 (s), 540 (m). UV/ Vis: 210 nm, 240 nm ,270 nm, 360 nm, 460 nm.

Synthesis of Di[{2,2-{benzene-1,4-diylbis[(E)methylylidene(1E,2E)hydrazine-2,1-diylidene (E)methylidene]} diphenolatenickel(II) (Ni-BHMD)

Yield: 84%. Elemental analysis; $C_{48}H_{42}NiN_8O_8$ (M.Wt: 917.026), Theo: C (62.7 %), N (12.21 %), O (13.9 %), H (4.10 %), Exp: C (62 %), N (12 %), O (13.20 %), H (4.01 %). FTIR analysis: 2954 (w), 1620 (s), 1456 (w), 1409 (w), 1300 (w), 1259.52 (s), 1213.23 (s), 1168.68 (m), 1078.21 (m), 952.84 (s), 831.32 (s), 734.88 (s), 675.09 (w), 563.21 (m), 549.71 (s), 430 (w). UV/ Vis: 205 nm, 220 nm, 245 nm, 350 nm, 470 nm.

Synthesis of Di[{2,2-{benzene-1,4-diylbis[(E)methylylidene(1E,2E)hydrazine-2,1-diylidene (E)methylidene]} diphenolatecopper(II)] (Cu-BHMD)

Yield: 88 %. Elemental analysis; $C_{48}H_{42}CuN_8O_8$ (M.Wt: 921.336), Theo: C (62.51 %), N (12.15 %), O (13.89 %), H (4.59 %), Exp: C (62.51 %), N (12.15 %), O (13.03%), H (4.1 %). FTIR analysis: 3300 (b), 2954 (w), 1678 (w), 1602 (s), 1462 (w), 1435 (s), 1244 (s), 1207 (s), 1080 (m), 991 (m), 858 (m), 734 (s), 560 (w). UV/ Vis: 220nm, 235nm, 280nm, 350nm.

Synthesis of Di[{2,2-{benzene-1,4-diylbis[(E)methylylidene(1E,2E)hydrazine-2,1-diylidene (E)methylidene]} diphenolatezinc(II) (Zn-BHMD)

Yield: 86%. Elemental analysis; $C_{48}H_{42}ZnN_8O_8$ (M.Wt: 923.716), Theo: C (62.4 %), N (12.13 %), O (13.9 %), H (4.08 %), Exp: C (62 %), N (12 %), O (13.97 %), H (4.08 %). FTIR analysis: 2954 (w), 1680 (w), 1620 (s), 1440 (w), 1338 (w), 1244 (s), 1211.30 (s), 1170 (w), 1026 (w), 958 (m), 831 (m), 779 (w), 734.88 (w), 580 (w), 567 (m), 522 (s), 467 (w). UV/ Vis: 210 nm, 230 nm, 250 nm, 360 nm.

Physical measurement

Solubility and melting point

The solubility of the prepared compounds was checked in many solvents including dimethylformamide (DMF), water, acetone, methanol, toluene, n-hexane, THF, dichloromethane, ethanol, benzene, chloroform, DMSO and acetonitrile. The melting point was found by using a small capillary tube in gallen kamp. The solubility and melting points are given below in table 1.

UV-Visible analysis

The Schiff base and its complexes are not soluble in most organic and inorganic solvent however Schiff base show solubility in tetrahydrofuran while complexes are soluble in different solvent. Two complexes show partial solubility in DMSO and two are fully soluble in THF. Few milli grams of Schiff base and its complexes were dissolved in minimum amount of their corresponding solvent in some clean and neat separate beakers. Electronic spectra of the analyte were obtained in DMSO and THF solvent in the range of 200-800 nm with DMSO and THF as a reference solvents.

Choice of solvents

The following criteria is considered while choosing a solvent for ultraviolet and visible spectroscopy.

1. The solvent should not captivate ultraviolet and visible energy in the same area as the substance whose spectrum is to be analyzed. Solvents without conjugated systems are most fit for this purpose.
2. The fine structure of absorption band should not be effect by the solvent. In non-polar solvent fine structure is often observed because it does not form hydrogen bond with the samples while in polar solvent the fine structure may vanish.

The third criteria are the solvent ability to effect the wavelength of UV energy will be absorbed via maintenance of either the ground or the excited state. In some case, polar solvent does not form stronger hydrogen bond with the excited state of polar sample as with their ground states and therefore $n\text{-}\pi^*$ type transition would take place at shorter wavelength. On the other hand, when the excited state form stronger hydrogen bond with the polar solvent then $\pi\text{-}\pi^*$ type transition would take place at longer wavelength [9].

FTIR analysis

H_2-BHMD Schiff base ligand and its metal complexes (M^{2+}: Co, Cu, Ni and Zn) were colored solid in nature. The samples were transformed into powdered form and FT-IR spectra, in the range of 4000-400cm^{-1}, were recorded.

Table-1: Solubility and melting points of the synthesized compounds.

S. NO	Compounds	Color	Solubility	Melting point (^{0}C)
1	Hydrazone	Yellow	Methanol, THF, DMSO	182
2	H_2-BHMD	Light yellow	THF (F), DMSO (P)	270
3	Zn-BHMD	Orange	DMSO (P, T)	>300
4	Cu-BHMD	Black	DMSO (P, T)	>300
6	Ni-BHMD	Brown	DMSO (P, T)	>300
8	Co-BHMD	Black	DMSO (P), THF (F)	>300

DMSO: Dimethyl sulfoxide THF: Tetrahydrofuran P: partially soluble F: fully soluble T: Soluble over heat

Thermogravimetric analysis

The Schiff base and its complexes are isolated as colored solid.TG/DTA instrument was used for the thermal and kinetic properties of the complexes at heating rate 10 $^{\circ}C$ min^{-1} in temperature range 30-1000 $^{\circ}C$. Definite mass of complexes were contained in ceramic pots vessels accustomed on platform giving a proportional indication to recorder, detected by computer interface and the results were plotted in the form of Δm of sample vs. temperature for TGA. All results were referenced to the thermal decomposition of alumina. ΔE was calculated for all complexes by using Horowitz-Metzger method.

When ln ln $(W_{0-} W_t^f / (W- W_t^f)$ were plotted against θ, then straight line was obtained, the slope of which was used for ΔE calculation by using the following expression;

$$Slope = E^*/ RT_s^2$$

Where

E^* = Activation energy
T_s= Temperature of max. weight loss
R = Universal gas constant

While $\theta = T_c-T_s$, W_0 = Initial mass, W = Weight remaining at T, W_t^f = Final weight, T_c = Specific temperature and T_s = Temperature of maximum weight loss. The activation energy terms hence calculated were further used for calculating the thermodynamic parameters like enthalpy, entropy and Gibb's free energy using the below expressions [10];

$$\Delta S^* = 2.303 \log [Ah/ KbT_s] R$$
$$\Delta H^* = \Delta E^* - RT$$
$$\Delta G^* = \Delta H^* - T\Delta S^*$$

Atomic absorption spectroscopy

The analysis of liquid samples by AAS is very easy, but it must be filtered prior to analyses. When sample is solid in nature, it must be converted into liquid form. As in present case, all metal complexes are colored solid, therefore fresh solution must be prepared for determination of metal content. 7 ppm/50ml fresh solutions of Ni, Co, Cu and 2ppm/50ml fresh solution of Zn metal complex were prepared in neat and clean separate beakers with the help of 8-10 ml concentrated nitric acid and distilled water. The nitric acid is used for digestion of the metal complexes. The complexes will break down into their respective components upon addition of conc. HNO_3. Similarly, the standard solution of the same metal with the same concentration was prepared and absorption of the sample solution was recorded in ppm unit [11].

Antioxidant activity

The DPPH scavenging activity is a standard test in antioxidant studies offering valuable method to test the radical scavenging power of a large number of compounds or extracts in chemical analysis. The extent to which a substance act as good antioxidant is depending upon the stable radical that is generated by providing labile hydrogen as a radical to the DPPH [12]. Blois developed a method for the determination of free radical scavenging assay.

500 ppm stock solution of Schiff base and its complexes were prepared by dissolving 2.5 mg samples in 5 ml DMSO/methanol (1:1 ratio). From the stock solution, five dilutions of different concentration like 10, 20, 30, 40 and 50 ppm were prepared. DPPH is a standard molecule whose solution was prepared by dissolving 1.57 mg DPPH in 20 ml DMSO. 50 µl of DPPH was added to each dilution. The final solution was left to stand for 30 min at 25 $^{\circ}C$ in darkness. Similarly, take 5 ml DMSO/methanol (1:1 ratio) in another separate neat and clean beaker and add to it 50 µl DPPH solution to prepare control solution. The blank solution was prepared by taking 5 ml DMSO/ methanol (1:1) solution. The absorbance of all prepared solutions was observed at 517 nm after incubating the solution for 30 min, then the given equation was used for calculation of antioxidant activity. All the experiments were performed three times for accuracy [13].

$$\% \text{ inhibition} = [A_c - A_s] \times 100 \div [A_c]$$

Result and Discussion

FTIR and ^{1}HNMR study of H_2-BHMD and its metal complexes (M-BHMD)

N_2O_2 type Schiff base ligand which are tetra dentate in nature was produced by reacting together hydrazone with O-vaniline. The IUPAC name of the ligand is 2,2- {benzene-1,4-diylbis [(E) methylylidene(1E,2E) hydrazine-2,1-diylidene (E) methyl idene]} diphenol (H_2-BHMD). The ligand has two anionic and two neutral sites of attachment. The comparison of IR spectra of the complexes and free ligand help in studying the changes that happened during the complexation process. It delivers

information about the functional group and metal–ligand bond formation.

The main FT-IR bands of the compounds are tabulated in table 2. The ligand shows strong absorption at 1247 cm^{-1} which was assigned to carbon-oxygen single bond of the phenolic group [14]. This band was shifted negatively by 3-7 cm^{-1} for all complexes except Ni-BHMD. In this complex, the band was shifted positively about 12 cm^{-1}. All these changes show that the oxygen atom of the phenolic group was involved in coordination with transition metal ions [15]. The spectra of ligand and complexes have peaks at 1460-1440 cm^{-1} due to benzene ring [16]. Strong absorption at 1620 cm^{-1} was observed in the H_2-BHMD Schiff base ligand spectrum. This was assigned to azomethine group -C=N-. The peak at this position also confirms the formation of Schiff base ligand. The stretching frequency of (O-H) bond in the free ligand is predictable at ν (3300–3800 cm^{-1}), but the frequency is generally emigrant to lower frequency due to the intramolecular hydrogen bonding (OH------N=C) in the H_2-BHMD Schiff base ligand. A broader band was observed for O-H bond, occasionally not detected for a stronger hydrogen bond.

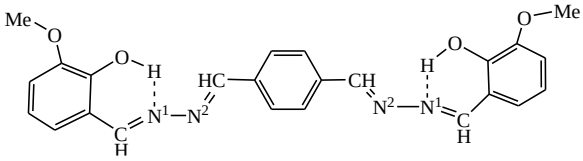

Fig 2: Formation of strong hydrogen bond in Schiff base ligand H_2-BHMD

Strong hydrogen bonds in these Schiff bases are usually observed because such Schiff bases are fairly planar with suitable intramolecular distances, thus helping in the formation of the strong hydrogen bond (Fig 2). A change in the position of intramolecular hydrogen bond does not take place even at high dilution because a change in concentration does not alter the internal bonding [17].

The methoxy group is electron donating group present on the phenolic ring. It would make the H----^{1}N hydrogen bond stronger, as seen in the Fig 2 [18]. The band of (-C=N-) in Zn-BHMD and Ni-BHMD complexes shifted to higher wave number suggesting that azomethine group taking part in bonding. The band of (-C=N-) in Cu-BHMD and Co-BHMD complexes shifted to lower wave numbers which may be credited to the bonding of the nitrogen with metal ions [19].

Convincing evidence for the formation of metal-ligand bonding has been observed in the spectra of metal complexes as new bands appeared at ν(567-540cm^{-1}) and at ν (420-520 cm^{-1}) which were assigned to ν(M-N) and ν(M-O) stretching vibrations respectively [20]. Therefore, the above discussion confirmed the formation of complexes. The ligand form bonds with the metal ions through nitrogen of -C=N- moiety and through oxygen of phenolic group. The formation of the ligand was further affirmed by ^{1}H-NMR. The HC=N peak was observed around 8.84 ppm as singlet. Whereas the peak for OH group was seen at 11.02 ppm. The OCH_3 proton appeared at 3.82 ppm. Rest of the spectrum was assigned to the respective aromatic protons. A polymer type compound was formed as may be seen in Fig 1. The polymeric nature was further confirmed by the solubility of metal complex. All complexes show poor solubility in common organic solvent except in THF and DMSO.

Table-2: FT-IR spectra (cm^{-1}) of H_2-BHMD ligand and M-BHMD complexes.

s: strong w: weak m: medium M: metal vw: very weak b: broad

Compounds	ν(sp^3 C-H)	ν(C=N)	ν(C-O)	ν(M-O)	ν(M-N)	ν(H_2O/ OH)
H_2-BHMD	2939vw	1618s	1247s	---------	---------	3440w
Zn-BHMD	2940vw	1620s	1244s	460m	567m	---------
Cu-BHMD	2939w	1602s	1240s	420s	560m	3300b
Ni-BHMD	2939w	1620s	1240w	430m	563m	---------
Co-BHMD	2954w	1602m	1242s	520s	540m	3398b

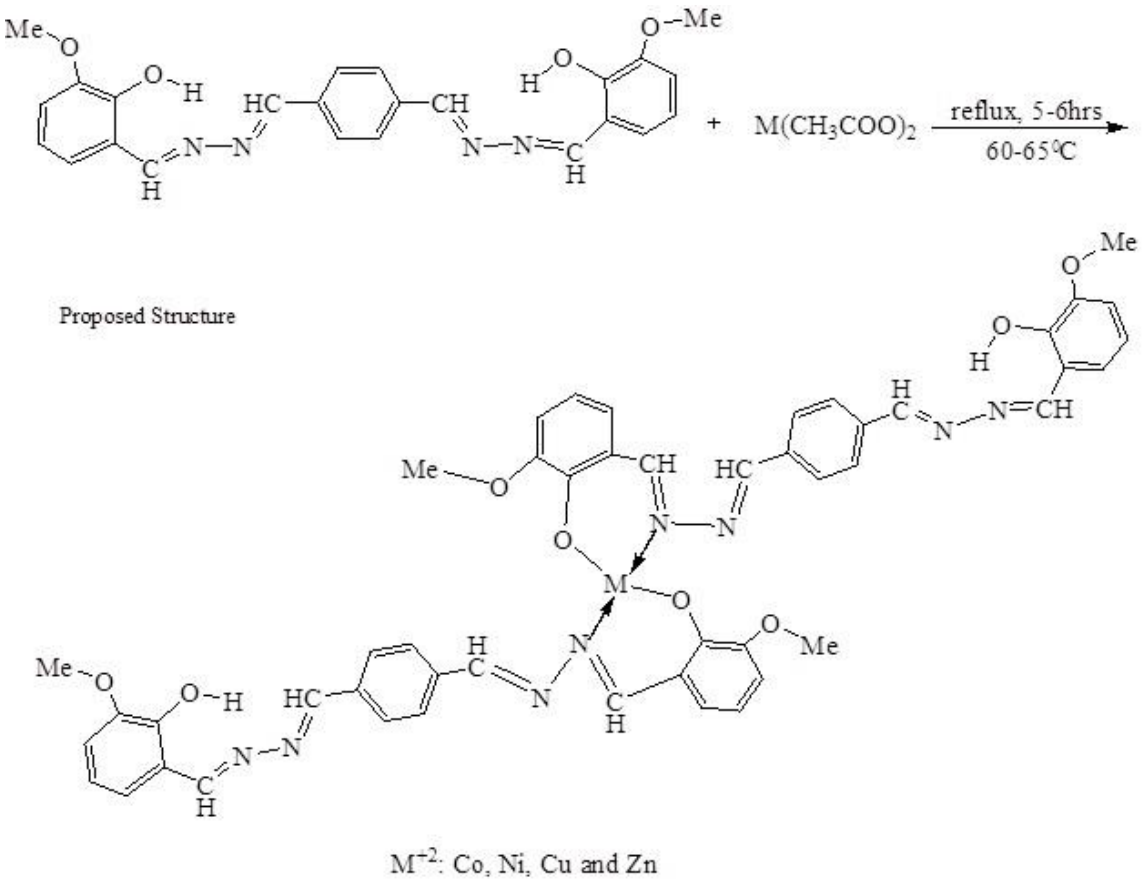

Scheme-3: Metal complexation of hydrazine Schiff base ligand (H_2-BHMD).

UV/ visible study of H_2-BHMD and its metal complexes (M-BHMD)

Many chromophoric centers have been observed in H_2-BHMD ligand. Five peaks in the UV region while two peaks in visible region were observed in Co-BHMD complex spectra. The peaks in UV region were assigned to the chromophore of H_2-BHMD ligand and the peaks in visible region i.e. 360nm and 460nm was assigned to the absorption by metal complex. The absorption at 360nm bring transition caused by $^2A_2 \rightarrow {}^2A_1$. The absorption at 360nm was very weak and it is forbidden. The absorption at 460nm was strongly observed and it is allowed. The band at 460nm was assigned to $^2A_2g \rightarrow {}^2B_1g$ transition. The crystal field splitting energy for this band was calculated to be 2.69 ev. The high CFSE is responsible for splitting of dyz and dxy orbital. Hence the Co-BHMD adopt distorted square planar geometry [21].

For Ni-BHMD five bands were observed viz; at 205 nm, 220 nm, 245 nm, 350 nm and 470 nm. The three bands observed in UV region were assigned to H_2-BHMD based absorption. While the two bands at 350 nm and 470 nm were assigned to transitions due to Ni-BHMD metal complex. The band at 470 nm was assigned to $^1A_1g \rightarrow {}^1A_2g$, since the absorption is predominantly charge transfer and observed strongly. The absorption at 350 nm was assigned to $^1A_1g \rightarrow {}^1B_1g$. The band $^1A_1g \rightarrow Eg$ is embedded in $^1A_1g \rightarrow {}^1B_1g$. The crystal field splitting energy for absorption at 470 nm was calculated to be 2.63 ev which is almost equal to CFSE for Co-BHMD. Therefore, same geometry will be assigned to Ni-BHMD complex. The only absorption at 350 nm in Cu-BHMD complex was assigned to $^2E \rightarrow {}^2T$. Rest of the spectrum was assigned to the absorption by Schiff base ligand. Overall, it can be concluded that diphenolate ion donates pi electrons to the metal center. These electrons are transferred to the metal and accommodated in $d\pi^*$ orbitals. The electrons from -C=N are also involved in bonding but the absorption caused by them are weakly observed. Hence some absorption is caused by phenolate group whereas others by Schiff base linkages. Zn-BHMD

was also assigned distorted square planar geometry as shown in scheme 3 [22].

Antioxidant activity of H_2-BHMD ligand and M-BHMD complexes

Structurally, DPPH has an odd electron and therefore it is paramagnetic in nature. The odd electron is delocalized over the whole molecule therefore it is a stable radical. It can be reduced by accepting an electron or hydrogen radical to become a stable diamagnetic spin-paired molecule. DPPH has maximum absorbance at 517 nm but upon reduction, a decrease in absorbance has been observed for DPPH radical and this is the reason that purple color of DPPH changes to yellow color. This decrease in absorbance is stoichiometric with the number of electrons or hydrogen radical taken up in a chemical reaction [23]. In the present study, the ligand present poor performance while testing as antioxidant. The poor performance may be due to two hydroxyl group which are involved in strong H-bonding, therefore it is not available for scavenging the DPPH radical. However, the metal complexes were rich in activity in comparison to the ligand, because now the hydroxyl groups are involved in bonding with metal ions. Only imine linkages remain to interact with DPPH radicals. The ligand and metal complexes show poor activity as a radical scavenger when compared with ascorbic acid.

There are a large number of literature reports showing good antioxidant activity of the ligand and upon complexation, its antioxidant activity increases tremendously [24]. In the present work, a linear relationship has been observed between the sample concentrations and inhibition activities. High antioxidant activity was observed when sample concentration was increased [25-28]. However, copper complex shows anomalous behavior. Up to 30 ppm, its inhibition activity was high, at 40 ppm its activity was low and again its activity was high at 50 ppm. Ni complex was the poorest complex among them, in term of inhibition activity. It's inhibition activity was almost just like the parent ligand. The cobalt complex shows highest inhibition activity up to 40 ppm as compared to the other complexes. The ligand and its Zn complex show linear relation in term of concentration and inhibition. In terms of inhibitory values it may be seen that the ligand H_2-BHMD shown 55ppm IC_{50} value whereas the corresponding Co-BHMD, Ni-BHMD, Cu-BHMD and Zn-BHMD revealed 32.66, 245.0, 51.11 and 46.84 IC_{50} values respectively. Overall, the activity is in the order:

Co-BHMD>Zn-BHMD>Cu-BHMD>H_2-BHMD>Ni-BHMD. Nickel complex is very poorly active in comparison to the parent ligand and other metal derivatives of the same ligand. The poor activity of the ligand may be assigned to the intra and intermolecular hydrogen bonding predominantly present in H2-BHMD. Whereas, in metal analogs the hydrogen bonding is overcome by coordination with metal centers. The results are tabulated in the table 3.

Table-3: Antioxidant activity of H_2-BHMD ligand and M-BHMD complexes.

S. No	Sample	Conc. (ppm)	Absorbance	% inhibition	IC_{50} (ppm)
		10	0.013	23	
		20	0.012	29	
1.	H_2-BHMD	30	0.011	35	55.00
		40	0..010	41	
		50	0.009	47	
		10	0.013	23	
		20	0.012	29	
2.	Zn-BHMD	30	0.011	35	46.84
		40	0.009	47	
		50	0.008	52	
		10	0.012	29	
		20	0.012	29	
3.	Cu-BHMD	30	0.010	41	51.11
		40	0.009	47	
		50	0.009	47	
		10	0.014	17	
		20	0.013	23	
4.	Ni-BHMD	30	0.011	35	245.0
		40	0.013	23	
		50	0.013	23	
		10	0.011	35	
		20	0.009	47	
5.	Co-BHMD	30	0.008	52	32.66
		40	0.007	58	
		50	0.008	52	
		10	--	53.96	
		20	--	60.18	
6.	Standard	30	--	68.40	3.84
		40	--	74.73	
		50	--	80.01	

Kinetic and thermodynamic studies

All the metal complexes were degraded thermally under air in the temperature range 30-1000 °C. Horowitz-Metzger strategy was used for calculation of kinetic and many thermodynamic parameter of the metal complexes. When the data points for lnln $[W_0-W_t^f/W-W_t^f]$ were plotted versus θ, linear plots were obtained. Co-BHMD was thermally degraded in two stages. The first stage of degradation was started at 30 °C and finish at 410 °C while the second stage start at 410 °C and finish at 800 °C. Beyond 800 °C residue of the metal oxide were observed. From the table 4, it becomes clear that the temperature at which maximum weight loss take place are 373 °C and 873 °C. ΔE, ΔH and ΔS for 1st stage was found to be 1.15 KJ/ mol, -2 KJ/ mol, -160 KJ/ mol respectively (table 4). ΔG was also not high for 1st stage. Therefore, the degradation of Co-BHMD in first stage is rather easy.

The ease of degradation may be ascribed to the breakage in polymeric chain. By looking into table 4, it may be concluded that activation energy is negative (E^* = -190 KJ/ mol). Whereas, the thermodynamic parameters like Gibb's free energy is also comparatively higher revealing that upon increase in temperature there is no adequate increase in reaction rate. Therefore, the second stage of decomposition is stable then the first stage; where, the single unit of metal complexes is likely to decompose.

The complex Ni-BHMD also decomposes in two stages of degradation i.e; the 1st stage starts at 257 °C and ends at 320 °C. The T_s for the first stage was found to be 623 °C whereas for the second stage is 923 °C. By looking into table 4.2, it is apparent that ΔE for the first stage of degradation is 52 KJ/mol higher than the activation energy for second stage. Similar trend may be seen in thermodynamic terms like enthalpy and entropy. Therefore, decomposition in first stage is slow but more stable than the second stage. The Gibb's free energy term show exergonic nature of the first stage compared to the second stage. By comparing the kinetic and thermodynamic terms of Co-BHMD and Ni-BHMD, Nickle based metal complex is far more stable than Co-BHMD and is unlikely to degrade.

The Cu-BHMD also decompose in two stages starting around 277°C and ends at 695 °C. Beyond 695 °C residue of CuO is observed. The first stage of degradation lies within the temperature range 270 °C to 300 °C. The activation energy term for the stage was found to be 1.3 KJ/ mol. The enthalpy value is equal to -2.98 KJ/ mol sharing the exothermic nature of the stage. The second stage of degradation is marked by 9.4 KJ/ mol activation energy, 3.8 KJ/ mol enthalpy, -197 KJ/mol entropy and 132 KJ/ mol Gibb's free energy (table 4). The enthalpy value and positive Gibb's free energy points to the endergonic nature of the intermediates produced. The large activation energy also marks the stable nature. Therefore, the polymeric coordination compound may here undergone changes to the stable complex. The Zn-BHMD also decompose in two stages of decomposition starting around 250 °C. The first stage of decomposition lasts for 240-500 °C encompassing another stage which is non separable. The second stage of decomposition starts around 500 °C and ends at 800 °C.

Beyond 800 °C the straight curve for the Zinc oxides as residue is obtained. The first stage of degradation was found with 2.31 KJ/ mol activation energy, -0.78 KJ/ mol enthalpy, 64 KJ/ mol Gibb's free energy and -173 KJ/ mol entropy. The kinetic and thermodynamic parameters represent exothermic nature of the 1st stage of degradation. By comparing the second stage of degradation it may be seen that E^* = 0.75 KJ/ mol, ΔH = -4.84 KJ/ mol, ΔG = 119 KJ/ mol and ΔS = -178 KJ/ mol. The activation energy and entropy terms are lower whereas Gibbs free energy term is larger than the first stage, therefore like the other metal complexes of the same ligand the intermediate produced during degradation are much more stable than the parent complex. Overall, the order of stability for the metal complexes may be assigned to vary in the order Ni> Co> Cu = Zn (1st order of degradation) and Ni> Co> Cu = Zn. From these orders it may be concluded that nickel based metal complex of H_2-BHMD are more stable than the other metal based complexes. Zinc based complexes are less liable to polymerize. Zn-based complex also tends to adopt tetrahedral geometry but here Zn is restricted to square planar environment which may be considered another reason for the unstable nature of the Zn-BHMD. The order of decreasing activation energy is Ni> Zn> Cu> Co (1st stage) and Ni> Cu> Zn> Co (2nd stage). Again both the orders are led by nickel based metal complex. Therefore, it may be concluded that nickel tends to adopt square planar geometry and is more likely to produce stable complex with H_2-BHMD ligand [29].

Table-4: Kinetic and thermodynamic parameters of H2-BHMD based metal complexes.

Compound	Stage of degradation	Ts in K	ΔE* (kJ/mol)	ΔH (kJ/mol)	ΔS (J/mol)	ΔG (kJ/mol)
Co-BHMD	**1st**	**373**	**1.15**	**-2.00**	**-160**	**60.0**
	2nd	**873**	**-190**	**-197**	**-184**	**161**
Ni-BHMD	**1st**	**623**	**52.0**	**44.0**	**-263**	**164**
	2nd	**923**	**28.0**	**21.0**	**-202**	**186**
Cu-BHMD	**1st**	**523**	**1.30**	**-2.98**	**-183**	**95.0**
	2nd	**673**	**9.40**	**3.80**	**-197**	**132**
Zn-BHMD	**1st**	**373**	**2.31**	**-0.78**	**-173**	**64.0**
	2nd	**673**	**0.75**	**-4.84**	**-178**	**119**

Conclusion

2,2-{benzene-1,4-diylbis[(E) methylylidene(1E, 2E) hydrazine-2,1-diylidene (E) methylidene]} diphenol (H_2-BHMD) is a hydrazone based Schiff ligand, was synthesized and characterized. It was further treated with first row transition metal ions like Co (II), Ni (II), Cu (II) and Zn (II) (hydrated acetate salt) for complexes preparation. The complexes were coordinated through four sites of attachment and adopted distorted square planar geometry. The geometries were assigned on various spectroscopic and analytical methods. Hydrazone Schiff base derivatives may offer active sites for the absorption of free radicals as evident from literature therefore, the metal derivatives and ligand were tested for their antioxidant activities using DPPH free radicals. It was found that all complexes show poor activity against DPPH except for Co-BHMD.

The metal complexation often enhances the stability of ligands therefore the metal derivatives were thermally cleaved in the temperature range 30-1000 ^{0}C in air. It was observed that the order of stabilities for 1st and 2nd stages of degradation were Ni> Co>Cu=Zn and Ni>Co>Cu=Zn respectively. Similarly, the order for decreasing activation energies for 1st and 2nd stages of degradation were Ni> Zn> Cu> Co and Ni> Cu> Zn> Co respectively. Both the orders suggest that Ni-BHMD metal complex are stable in nature.

Conflict of Interest

The authors of this manuscript declare no conflict of interest.

References

1. W. H. Mahmoud, R.G. Deghadi, G.G. Mohamed, Spectroscopic and thermal characterization of biologically and anticancer active novel Schiff base metal complexes. *Res. Chem. Intermed.* **42**, 7869, (2016).
2. H.S.V. Jois, B. Kalluraya, T. Vishwanath, Synthesis, Spectroscopic Properties and Antioxidant Activity of Bis-Hydrazones and Schiff's bases Derived from Terephthalic Dihydrazide. *J. Fluoresc.* **25**, 481, (2015).
3. H. Temel, H. Hosgoren New copper(II), manganese(III), nickel(II) and zinc(II) complexes with a chiral quadridentate Schiff base, *Transit. Met. Chem.* **27**, 609, (2002).
4. M. Ikram, S. Rehman, F. Subhan, M. N. Akhtar, M. O. Sinnokrot, Synthesis, characterization, thermal degradation and urease inhibitory studies of the new hydrazide based Schiff base ligand 2-(2-hydroxyphenyl)-3-{[(*E*)-(2-hydroxyphenyl)methylidene]amino}-2,3-dihydroquinazolin-4(1*H*)-one, *Open Chem.*, **15**, 308, (2017).
5. A.A. Al-Amiery, Synthesis and antioxidant, antimicrobial evaluation, DFT studies of novel metal complexes derivate from Schiff base, *Res. Chem. Intermed.* **38**, 745, (2012).
6. R. Golbedaghi, R. Fausto, Coordination aspects in Schiff bases cocrystals, *Polyhedron*, **155**, 1, (2018).
7. J. Liu H. Pu, S. Liu, J. Kan, C. Jin, Synthesis, characterization, bioactivity and potential application of phenolic acid grafted chitosan: A review, *Carbohydr. Polym.* **174**, 999, (2017).
8. M. Ikram, S. Rehman, Faridoon, R.J. Baker, H.U. Rehman, A. Khan, M.I. Choudhary, S.U. Rehman, Synthesis and distinct urease enzyme inhibitory activities of metal complexes of Schiff-base ligands: Kinetic and thermodynamic parameters evaluation from TG-DTA analysis, *Thermochim. Acta*, **555**, 72, (2013).
9. D.L. Pavia, G.M. Lampman, G.S. Kriz, Introduction to spectroscopy, 5th edition, ISBN: 0-03-031961-7, (2013).
10. N. Muhammad, M. Ikram, S. Rehman, M. Ibrahim, Viola, C. Schulzke Structural, thermal kinetics and thermodynamics study of new mixed ligand zinc complexes, *J. Therm. Anal. Calorim.* **128(1)**, 627, (2017). DOI 10.1007/s10973-016-5842-7.
11. Y. Anjaneyulu, K. Chandrasekhar, V.A. Manickman, Text Book of Analytical Chemistry, Chapter 23: Atomic Emission, Fluorescence and Absorption Spectroscopy, 463, (2006).
12. S.J. Kirubavathy, S. Chitra, Structural, theoretical investigations and biological evaluation of Cu(II), Ni(II) and Co(II) complexes of mercapto-pyrimidine Schiff bases, *J. Mol. Struc.* **1147**, 797, (2017).
13. Q. M. Hasi, Y. Fan, X. Feng, X. Yao, J. Liu, Antioxidant and antimicrobial properties of nickel(II), cobalt(III), and zinc(II) complexes of a Schiff base ligand, *Transit. Met Chem.*, **41**, 685, (2016).
14. Y. Zhao, Z. Li, H. Li, S. Wang, M. Niu, Synthesis, crystal structure, DNA binding and in vitro cytotoxicity studies of Zn(II) complexes derived from amino-alcohol Schiff-bases, *Inorg. Chim. Acta*, **482**, 136, (2018).
15. R. Olar, M. Badea, M. Ferbinteanu, N. Stanica, I. Alan, Spectral, magnetic and thermal characterization of new Ni(II), Cu(II), Zn(II) and Cd(II) complexes with a bischelate Schiff base,

J. Therm. Anal. Calorim. **127(1)**, 709, (2017). DOI 10.1007/s10973-016-5433-7.
16. Pavia, lampman, kriz. Infrared spectroscopy, Introduction to spectroscopy, third edition, ISBN: 0-03-031961-7, 47-48, (2001).
17. N.K. Gondia, S.K. Sharma, Spectroscopic characterization and photophysical properties of schiff base metal complex, *J. Mol. Struc.* **1171**, 619, (2018).
18. B. Ambrozini E.R. Dockal, T.G. Cavalheiro, Thermal behavior of tetradentate Schiff base chromium(III) complexes, *J. Therm. Anal. Calorim.* **115**, 979, (2014).
19. R.H. Huia, P. Zhoua and Z.L. You, Syntheses, Characterization, and Crystal Structures of Two Dinuclear Nickel(II) and Copper(II) Complexes with Schiff Bases, *Russ. J. Coord. Chem.* **36**, 525, (2010).
20. S. Akine, T. Nabeshima, Increased Nuclearity of Salen‐Type Transition Metal Complexes by Incorporation of O‐Alkyloxime Functionality, *Heteroat. Chem.* **25**, 410, (2014).
21. M. Ikram, S. Rehman, A. Khan, R.J. Baker, T.S. Hofer, F. Subhan, M. Qayum, Faridoon, C. Schulzke, Synthesis, characterization, antioxidant and selective xanthine oxidase inhibitory studies of transition metal complexes of novel amino acid bearing Schiff base ligand, *Inorg. Chim. Acta,* **428**, 117, (2015).
22. E. Yousif, A. Majeed, K. Sammarrae, N. Salih, J. Salimon, B. Abdullah, Metal Complexes of Schiff base: Preparation, characterization and antibacterial activity, *Arab. J. Chem.* **10**, S1639, (2017).
23. D.A. Patel, A.A. Patel, H.S. Patel, Synthetic, spectroscopic, magnetic and thermal aspects of drug based metal complexes derived from 1st row transition metal ions, *Arab. J. Chem.* **10**, S2217, (2017).
24. S. B. Moosun, S. Jhaumeer-Laulloo, E. C. Hosten, T. I. A. Gerber, M. G.. Bhowon, Antioxidant and DNA binding studies of Cu(II) complexes of N,N'-(1,10-dithio-bis(phenylene))-bis(salicylideneimine): synthesis and characterization, *Transit. Met. Chem.* **40**, 445, (2015).
25. M. Jafari, M. Salehi, M. Kubicki, A. Arab, A. Khaleghian, DFT studies and antioxidant activity of Schiff base metal complexes of 2-aminopyridine. Crystal structures of cobalt(II) and zinc(II) complexes, *Inorg. Chim. Acta,* **462**, 329, (2017).
26. O. A. EL-Gammal, H. A. Alshater, H. A. El-Boraey Schiff base metal complexes of of 4-methyl-1H-indol-3-carbaldehyde derivative as a series of potential antioxidants and antimicrobial: Synthesis, Spectroscopic Characterization and 3D molecular modeling *J. Mol. Struct.*, **1195**, 220, (2019)
27. H. A. El-Boraey, O. A. El-Gammal, N. G. Abdel Sattar, Impact of gamma ray irradiation on some aryl amide bridged Schiff base complexes: spectral, T`GA, XRD and antioxidant property, *J. Radioanal. Nucl. Chem.* **323**, 241, (2020).
28. H. A. El-Boraey, M. A. El-Salamony, Transition Metal Complexes with Polydentate ligand: Synthesis, Characterization, 3D Molecular Modeling, Anticancer, Antioxidant and Antibacterial Evaluation. *J. Inorg. Organomet. Poly. Mat.* **29**, 684, (2019).
29. M. Ikram, S. Rehman, M. Ali, Faridoon, C. Schulzke, R.J. Baker, A.J. Blake, K. Malook, H. Wong, S. Rehman, Urease And -Chymotrypsin Inhibitory Activities of Transition Metal Complexes of New Schiff Base Ligand: Kinetic and Thermodynamic Studies of the Synthesized Complexes Using Tg–Dta Pyrolysis, *Thermochim. Acta,* **562**, 22, (2013)